Mechanisms of DNA damage induced by morin, an inhibitor of amyloid β-peptide aggregation

Yurie Mori [a], Shinya Kato [b], Yutaka Fujisawa [c], Shiho Ohnishi [c], Yusuke Hiraku [a], Shosuke Kawanishi [c], Mariko Murata [a], Shinji Oikawa [a]*

[a] *Department of Environmental and Molecular Medicine, Mie University Graduate School of Medicine, Edobashi 2-174, Tsu, Mie 514-8507, Japan*
[b] *Radioisotope Facilities for Medical Science, Mie University, Edobashi 2-174, Tsu, Mie 514-8507, Japan*
[c] *Faculty of Pharmaceutical Sciences, Suzuka University of Medical Science, 3500-3, Minamitamagaki, Suzuka, Mie, 513-8670, Japan*

* Corresponding author at: Department of Environmental and Molecular Medicine, Mie University Graduate School of Medicine, Edobashi 2-174, Tsu, Mie 514-8507, Japan.
Tel./Fax: +81-59-231-5011
E-mail address: s-oikawa@doc.medic.mie-u.ac.jp (S. Oikawa)

Abstract

Morin is a potential inhibitor of amyloid β-peptide aggregation. This aggregation is involved in the pathogenesis of Alzheimer's disease. Meanwhile, morin has been found to be mutagenic and exhibits peroxidation of membrane lipids concurrent with DNA strand breaks in the presence of metal ions. To clarify a molecular mechanism of morin-induced DNA damage, we examined the DNA damage and its site specificity on ^{32}P-5'-end-labeled human DNA fragments treated with morin plus Cu(II). The formation of 8-oxo-7,8-dihydro-2'-deoxyguanosine (8-oxodG), an indicator of oxidative DNA damage, was also determined in calf thymus DNA treated with morin plus Cu(II). Morin-induced DNA strand breaks and base modification in the presence of Cu(II) were dose dependent. Morin plus Cu(II) caused piperidine-labile lesions preferentially at thymine and guanine residues. The DNA damage was inhibited by methional, catalase, and Cu(I)-chelator bathocuproine. The typical •OH scavengers ethanol, mannitol, and sodium formate showed no inhibitory effect on DNA damage induced by morin plus Cu(II). When superoxide dismutase was added to the solution, DNA damage was not inhibited. In addition, morin plus Cu(II) increased 8-oxodG formation in calf thymus DNA fragments. We conclude that morin undergoes autoxidation in the presence of Cu(II) via a Cu(I)/Cu(II) redox cycle and H_2O_2 generation to produce Cu(I)-hydroperoxide, which causes oxidative DNA damage.

Keywords

Morin, Copper, DNA damage, Reactive oxygen species,

8-oxo-7,8-dihydro-2’-deoxyguanosine

Introduction

Morin (2',3,4',5,5-pentahydroxyflavone) is a flavonol found in wine, many herbs, and fruits [1]. Multiple pharmacological effects of morin have been investigated including antioxidant activities [3, 4], cellular protection [5, 6, 7], anti-inflammatory [8, 9], and anti-fibrotic effects [10]. Recently, it has been found that morin is an effective anti-aggregation compound targeting the amyloid β-peptide [11]. The central dogma of the 'amyloid hypothesis' states that aggregation and deposition of the amyloid β-peptide in the brain are pathological phenomena in the progression of Alzheimer's disease [12]. By *in vivo* assay, intranasal administration of a morin-loaded emulsion improved the memory in Wistar rats with dementia [13]. Thus, morin is expected to be a possible prophylactic agent for Alzheimer's disease. However, in the presence of metal ions, morin induces peroxidation of nuclear membrane lipids concurrent with DNA strand breaks in isolated rat liver nuclei [14]. In addition, a synthesized morin-Cu(II) complex (2:1 mol/mol) is found to cleave plasmid DNA via an oxidative pathway and to inhibit the growth of human HeLa cells [15]. Furthermore, morin is found to be mutagenic in the Salmonella/microsomal activation system [16, 17], but the molecular mechanism of morin-induced DNA damage has not been elucidated sufficiently in relation to reactive oxygen species (ROS).

Our research interest involves assessing the biological properties of morin in relation

to DNA damage. In the present study, we aimed to clarify the molecular mechanism of morin-induced DNA damage in the presence of Cu(II). We examined morin-induced DNA damage in terms of ROS generation and its site specificity on DNA base sequences using human ^{32}P-5'-end-labeled DNA fragments. The formation of 8-oxodG, an indicator of oxidative DNA damage [18], was also determined in calf thymus DNA treated with morin using high performance liquid chromatography (HPLC) equipped with an electrochemical detector (ECD) [19]. In order to propose possible mechanism of DNA damage induced by morin and Cu(II), we analyzed oxidized product of morin by HPLC and NMR.

Materials and methods

Materials

Restriction enzyme *Bam*HI and T_4 polynucleotide kinase were purchased from New England Biolabs Ltd. (Ipswich, MA). Restriction enzyme *Mro*I was from Toyobo Co., Ltd. (Osaka, Japan), and *Bss*HII from Takara Bio Inc. (Shiga, Japan). [γ-^{32}P]ATP (222 TBq/mmol) was from PerkinElmer, Inc. (Waltham, MA). Diethylenetriamine-*N, N, N′, N″, N″*-pentaacetic acid (DTPA) and bathocuproinedisulfonic acid were from Dojindo Laboratories (Kumamoto, Japan). Superoxide dismutase (3,000 units/mg from bovine

erythrocytes, Cu/Zn) and catalase (30,000 units/mg from bovine liver) were from Sigma-Aldrich Co. LLC. (St Louis, MO). 3-(Methylthio) propionaldehyde (methional) and morin hydrate were from Tokyo Chemical Industry Co., Ltd. (Tokyo, Japan). Copper(II) chloride dihydrate ($CuCl_2 \cdot 2H_2O$), ethanol, mannitol, and sodium formate were from Nacalai Tesque (Kyoto, Japan). Nuclease P_1 (500 units/vial) and piperidine were from Wako Pure Chemical Co. Ltd. (Osaka, Japan). Calf intestinal phosphatase (500 units/vial) were purchased from Roche Diagnostics GmbH (Mannheim, Germany). All other reagents were commercial products of the reagent grade.

Preparation of ^{32}P-5'-end-labeled DNA fragments

DNA fragments containing exon 1 or 2 of the human *p16* tumor suppressor gene [20] were obtained by PCR amplification of human genomic DNA as described previously [21]. The DNA was dephosphorylated with calf intestinal phosphatase and phosphorylated with [γ-^{32}P] ATP and T_4 polynucleotide kinase to yield a 5'-end-labeled 490 base pair (bp) fragment (*Eco*RI* 5841-*Eco*RI* 6330) containing exon 1 and the 460 bp fragment (*Eco*RI* 9481-*Eco*RI*9940) containing exon 2. The 490 bp fragment was further digested with *Mro*I to obtain the singly labeled 328 bp fragment (*Eco*RI* 5841-*Mro*I 6168) and the 158 bp fragment (*Mro*I 6173-*Eco*RI* 6330). The 460 bp fragment was further digested with *Bss*HII to obtain the singly labeled 309 bp fragment

(*Eco*RI* 9481-*Bss*HII 9789) and the 147 bp fragment (*Bss*HII 9794-*Eco*RI* 9940). The asterisk indicates ^{32}P-labeling.

Analysis of DNA damage by morin in the presence of Cu(II)

The standard reaction mixture in a microtube contained morin, 20 μM $CuCl_2$, ^{32}P-5'-end-labeled DNA fragments, and 100 μM/base calf thymus DNA in 200 μL of 4 mM sodium phosphate buffer (pH 7.8) containing 5 μM DTPA. After incubation at 37 ºC for 5 hr, the DNA fragments were heated at 90 ºC in 10% piperidine for 20 min (piperidine treatment). The DNA fragments were then electrophoresed on an 8% polyacrylamide-8M urea gel (14 × 16 cm) and the autoradiogram was obtained by exposing an X-ray film (Fujifilm Corp., Tokyo, Japan) to the gel as previously described [22, 23].

The preferred cleavage sites were determined by direct comparison of the positions of the oligonucleotides with those produced by the chemical reactions of the Maxam-Gilbert sequencing method [24] using a DNA-sequencing system (LKB 2010 Macrophor, LKB Pharmacia Biotechnology Inc., Uppsala, Sweden). The reaction mixture in a microtube contained 500 μM morin, 20 μM $CuCl_2$, ^{32}P-5'-end-labeled DNA fragments, and 100 μM/base calf thymus DNA in 200 μL of 4 mM sodium

phosphate buffer (pH 7.8) containing 5 μM DTPA. After incubation at 37 ºC for 5 hr, followed by piperidine treatment, the DNA fragments were electrophoresed on an 8% polyacrylamide-8M urea gel (21×53 cm) and the autoradiogram was obtained by exposing an imaging plate (BAS-MS2040, Fujifilm Corp.) to the gel. The relative amounts of oligonucleotides from the treated DNA fragments were measured using a laser scanner (Typhoon FLA-9500, GE Healthcare, Buckinghamshire, England) and analyzed with ImageQuant TL software (GE Healthcare).

Analysis of 8-oxodG formation in calf thymus DNA by morin in the presence of Cu(II)

The 8-oxodG formation was determined by a modification of the method described by Kasai et al [25]. Calf thymus DNA fragments of 100 μM/base were incubated with morin and 20 μM $CuCl_2$ in 400 μL of 4 mM sodium phosphate buffer (pH 7.8) containing 5 μM DTPA for 1 hr at 37 ºC. Calf thymus DNA is a natural DNA widely used in physicochemical studies of DNA. After ethanol precipitation, the DNA fragments were digested to nucleosides with nuclease P_1 and calf intestinal phosphatase, and then 8-oxodG in DNA was analyzed by an HPLC system (SLC-10Avp, LC-20AD, SPD-10AVvp, Shimadzu Corp., Kyoto, Japan) equipped with an ECD (Coulochem III,

ESA Inc., Chelmsford, MA) as previously described [26]. Furthermore, in order to clarify the mechanism of autoxidation, dissolved oxygen in the reaction mixture containing morin and Cu(II) was removed by bubbling nitrogen gas for 1 min (hypoxic conditions), after which 8-oxodG was determined.

Analysis of reaction products of morin and Cu(II) by HPLC, ESI-MS and NMR

The Reaction mixture consisted 500 μM morin and $CuCl_2$ in 4 mM sodium phosphate buffer (pH 7.8) containing 5 μM DTPA. After incubation at 37 ºC for 21 h, the reaction mixture was analyzed by HPLC (Prominence LC-20A series, Shimadzu Corp., Kyoto, Japan) equipped with a UV/VIS detector. The mobile phase in HPLC consisted a mobile phase (A) 0.05 % TFA in water and a mobile phase (B) 0.05 % TFA in acetonitrile, the composition of which was varied employing the following HPLC gradient program: 0-5.0 min, 95 % A (isocratic); 5.1-25.0 min, 95 % -50 % A (linear gradient); 25.1 min, 5 % A; 25.1-30.0 min, 5 % A (isocratic); 30.1-45.0 min, 95 % A. The reaction mixture was separated by using a CAPCELL PAK C18 MG III column (4.6 mmID×150 mm, 5 μm, SHISEIDO). Other chromatographic conditions were as follows: flow rate of 1 ml/min and oven column set at 40 ºC.

The UV absorbance of the HPLC eluate was monitored at 254 nm and several peaks were detected increasing with dose-dependent of copper ions. The eluate containing the

most increased peak were collected and lyophilized overnight to confirm the structure of the oxidized product of morin.

The oxidized product was identified by using a NMR system 600 NB (Varian, Palo Alto, CA, USA) and a micrOTOF-Q ESI-quadrupole/time-of-flight tandem mass spectrometer (Bruker Co., Billerica, MA, USA). ^{1}H- and ^{13}C-NMR spectra of the oxidized product in DMSO-d_6 were recorded at 600 and 150 MHz at 20 ºC, respectively. All NMR spectra were referenced to tetramethylsilane. Distortionless enhancement by polarization transfer (DEPT) and two dimensional NMR experiments (^{1}H-COSY, proton correlation spectroscopy; HSQC, heteronuclear single-quantum correlation spectroscopy; HMBC, heteronuclear multiple-bond correlation spectroscopy) were performed to assist in assigning ^{1}H- and ^{13}C-NMR spectra of the oxidized product. Furthermore, the oxidized product was reconstituted in 50 % aqueous methanol or deuterium solvent to determine its molecular weight and the number of acidic protons in its structure by using ESI-MS and MS/MS.

Results

Damage to ^{32}P-labeled DNA fragments by morin in the presence of Cu(II)

Figure 1 shows an autoradiogram of the DNA fragments which were treated with various concentrations of morin in the presence of Cu(II), and were subsequently either subjected to piperidine treatment or subjected to no treatment. When treated with morin in the presence of Cu(II), DNA fragments were damaged, as shown in the autoradiogram (Fig. 1A and B). The intensity of the DNA damage increased with morin concentration when there was no treatment with piperidine (Fig. 1B). The DNA damage was further enhanced with piperidine treatment (Fig. 1A), indicating that the base alteration was caused by morin plus Cu(II) in addition to breakage of the deoxyribose phosphate backbone of DNA.

Effects of scavengers and bathocuproine on DNA damage induced by morin in the presence of Cu(II)

Figure 2 shows the effects of scavengers and bathocuproine on DNA damage induced by morin in the presence of Cu(II). The •OH scavengers ethanol, mannitol, and sodium formate did not inhibit DNA damage, whereas methional, which scavenges a variety of ROS in addition to •OH [27], was able to inhibit DNA damage. Catalase, which decomposes hydrogen peroxide (H_2O_2) [28] and bathocuproine, which is a Cu(I)-specific chelator [29], were also able to inhibit DNA damage. DNA damage was not inhibited by the addition of superoxide dismutase, which catalyzes the dismutation

of the superoxide anion radical ($O_2^{\bullet-}$) into oxygen (O_2) and H_2O_2.

Site specificity on DNA damage induced by morin in the presence of Cu(II)

The site specificity of DNA damage induced by morin in the presence of Cu(II) is shown in Fig. 3. Morin plus Cu(II) induced piperidine-labile sites at thymine (T), guanine (G), and cytosine (C) residues, but to a lesser extent at adenine (A) residues. Morin plus Cu(II) caused piperidine-labile sites preferentially at T in 5'-TG-3' and 5'-G in 5'-GGG-3' sequences.

Formation of 8-oxodG in calf thymus DNA treated with morin in the presence of Cu(II)

Figure 4 shows the 8-oxodG formation in calf thymus DNA by morin in the presence of Cu(II). The content of 8-oxodG in calf thymus DNA was increased by morin plus Cu(II) in a dose-dependent manner of morin. The 8-oxodG formation under hypoxic conditions was lower than that under normal conditions.

Oxidized products of morin and Cu(II) by HPLC, ESI-MS and NMR

Figure 5A shows a chromatogram of oxidized product of morin by HPLC. The peak at retention time (Rt) 14.8 min extensively increased with dose-dependent of $CuCl_2$.

Moreover, other peaks at Rt 5.6, 8.0 and 12.5 min also increased (Figure 5A). A molecular weight of the oxidized products detected at Rt 14.8 min was estimated by ESI-MS. We obtained mass spectrum at *m*/*z* of 155.0 (in methanol/H_2O=1/1) and 159.0 (in methanol-d_4/D_2O=1/1) in the positive scan mode by ESI-MS (data not shown). In the negative scan mode, we obtained spectrum at *m*/*z* of 153.0 (in methanol/H_2O=1/1), 155.0 (in methanol-d_4/D_2O=1/1) (data not shown). However, a molecular weight of the peak detected at Rt 5.6, 8.0 and 12.5 min could not be identified.

Figure 5B shows the ^{1}H- and ^{13}C-NMR spectra of the oxidized product of morin (the peak at Rt 14.8 min). Chemical shifts of the ^{1}H signals were obtained at δ 13.39 ppm (0.5 H, broad, COO*H*), 11.42 ppm (0.9 H, broad singlet, 2-O*H*), 10.37 ppm (1.0 H, singlet, 4-O*H*), 7.62 ppm (1.0 H, doublet, *J*= 8.4 Hz, 6-C*H*), 6.34 ppm (1.0 H, double doublet, *J*= 8.7 and 1.8 Hz, 5-C*H*), 6.26 ppm (1.0 H, doublet, *J*= 1.8 Hz, 3-C*H*). In addition, chemical shifts of the ^{13}C signals were obtained at δ 171.9 ppm (quaternary, *C*OOH), 163.9 ppm (quaternary, 4-*C*-OH), 163.3 ppm (quaternary, 2-*C*-OH), 131.8 ppm (tertiary, 6-*C*H), 107.8 ppm (tertiary, 5-*C*H), 104.2 ppm (quaternary, 1-*C*-COOH), 102.1 ppm (tertiary, 3-*C*H).

In these result, the peak at Rt 14.8 min was identified as 2,4-dihydroxybenzoic acid (Figure 5C).

Discussion

We investigated the mechanism of DNA damage induced by morin in the presence of Cu(II) using ^{32}P-labeled human DNA fragments. Our results indicated that morin plus Cu(II) caused DNA damage and this damage was dose-dependent on morin (Fig. 1). The morin-induced DNA damage was enhanced by piperidine treatment, suggesting that morin plus Cu(II) causes base alterations in addition to breakage of the deoxyribose phosphate backbone of DNA. These results suggest that Cu(II) is an important factor in the DNA damage induced by morin.

Roy *et al.* reported that a synthesized morin-Cu(II) complex (2:1 mol/mol) caused strand breaks in plasmid DNA [15], but site specificity in the DNA damage was not elucidated. Our results of site specificity determined by the Maxam-Gilbert sequencing method indicated that morin plus Cu(II) induced piperidine-labile sites at T, G, and C residues (Fig. 3). It is known that hot piperidine can cleave DNA strands at the labile base lesions of oxidative DNA-damaged bases including thymine glycol, 5-hydroxycytosine, oxazolone, and imidazolone [30]. Geierstanger *et al.* reported that Cu(II) is more likely to bind to G than to A in double-stranded DNA [31]. It is known

that metal ions bind more preferentially to poly G sequences than single G [32], and H_2O_2 produces ROS, which mediate DNA strand breaks at the 5'-G in GG and GGG sequences [33, 34]. In the present study, morin plus Cu(II) caused piperidine-labile sites preferentially at T in 5'-TG-3' and 5'-G in 5'-GGG-3' sequences, suggesting an underlying process in which Cu(II) binds to G and thereafter neighboring residues are damaged. On the other hand, it is well-known that free •OH causes DNA damage without site specificity [35]. Therefore, our results suggest that ROS other than •OH are involved in morin-induced DNA damage in the presence of Cu(II).

To clarify what kind of ROS cause the DNA damage, the effects of various scavengers were examined (Fig. 2). The typical •OH scavengers, ethanol, mannitol, and sodium formate showed no inhibitory effect on DNA damage induced by morin plus Cu(II). Superoxide dismutase, which catalyzes the dismutation of $O_2^{\bullet-}$ into O_2 and H_2O_2, did not inhibit the DNA damage. Meanwhile, the DNA damage was inhibited by catalase, suggesting that H_2O_2 participated in the DNA damage [28]. Bathocuproine also inhibited the DNA damage, suggesting that Cu(I) is involved in the DNA damage [29]. Methional inhibited the DNA damage, suggesting that the DNA damage is caused by a variety of ROS in addition to •OH [27]. Collectively, it is suggested that H_2O_2 and Cu(I) play an important role in the production of ROS, which are responsible for

morin-induced DNA damage in the presence of Cu(II).

To evaluate whether morin induces oxidative DNA damage, we determined the process of 8-oxodG formation, which is an indicator of oxidative stress to DNA [18]. The 8-oxodG formation in calf thymus DNA fragments was increased by treatment with morin in a dose-dependent fashion in the presence of Cu(II) (Fig. 4). When dissolved oxygen in the reactive solution containing morin and Cu(II) was removed by bubbling nitrogen gas, the 8-oxodG formation was decreased as compared to that where dissolved oxygen was not removed. Our results suggest a possible mechanism in which Cu(II) is reduced by morin to Cu(I) and concomitantly mediates ROS generation, resulting in oxidative DNA damage. Min *et al*. reported that 100 μM of morin enhanced 8-oxodG formation in calf thymus DNA in the presence of Fe(II) and H_2O_2 [36]. It is implicated that morin causes DNA damage through autoxidation reactions.

To determinate of the structure of oxidized product, we evaluated the ^{1}H-NMR spectrum, three proton signals observed in the chemical shifts from 8.0 to 6.0 ppm were indicated the characteristic signals of three-substituted benzene in the position of 1, 2 and 4. The integral value of a broad signal in the chemical shifts of 13.4 ppm were 0.52, which was suggested that this functional group possessed a higher acidic proton such as a carboxylic acid. Three signals observed in the chemical shifts from 14.0 to 10.0 ppm

disappeared by hydrogen/deuterium (H/D) exchange after addition of deuterium oxide. Furthermore, the results in ESI-MS experiments by using 50 % aqueous methanol or deuterium solvent were suggested that the oxidized product of morin possessed three H/D-exchangeable protons in the structure with a monoisotopic mass of 154.0 Da. Subsequently, a product ion scan of *m/z* 153.0 or 155.0, which was performed under negative polarity with collision-induced dissociation in MS/MS, produced decarboxylation ions with *m/z* of 109.0 or 111.0 (data not shown) from the corresponding precursor ions. These results in NMR, ESI-MS, and MS/MS experiments allowed us to identify the oxidized product of morin by Cu(II) ion as 2,4-dihydroxybenzoic acid.

Based on these results, we propose a possible mechanism of morin-induced DNA damage in the presence of Cu(II) as shown in Fig. 6. We presume that morin undergoes Cu(II)-mediated autoxidation to generate Cu(I) and a semiquinone radical at the position 4' on B-ring of morin; thereafter, Cu(I) and the semiquinone radical reacts with O_2 to generate $O_2^{\bullet-}$. Because an enol moiety in ring C (the hydroxy group in ring C) is conjugated to the 4' hydroxy group in ring B of morin, the semiquinone radical would be oxidized to the 3, 4-diketo form at ring C, and $O_2^{\bullet-}$ is reduced to H_2O_2. The autoxidation of morin is promoted in the presence of Cu(II) via a Cu(II)/Cu(I) redox

cycle and H_2O_2 generation. Concerning the mechanism of oxidative DNA damage in the presence of copper, previous studies indicated that Cu(I) binds to DNA and reacts with H_2O_2, resulting in the formation of Cu(I)-hydroperoxide [37, 38, 39, 40]. The Cu(I)-hydroperoxo complex may be considered to be a bound •OH, which can release •OH and lead to oxidative DNA damage [40]. Our results indicated that •OH scavengers could not inhibit morin-induced DNA damage in the presence of Cu(II). Based on these findings, the mechanism underlying morin-induced DNA damage in the presence of Cu(II) is probably due to the generation of •OH near the site of Cu(I) fixation at G on DNA bases [37, 41]. The •OH rapidly attacks the adjacent T and G residues prior to being scavenged by •OH scavengers [42]. This speculation is supported by previous studies which show that catechin and catechol are autoxidized to quinones in the presence of Cu(II) concomitantly with Cu(I)-hydroperoxide formation, and which show piperidine-labile sites preferentially at T and/or C neighboring G [40, 43].

In this study, *para*-quinone methide form of morin shown in Fig. 6 could not be detected due to its unstable structure in the reaction buffer. Kummer *et al.* reported that an oxidation of morin produced several nucleophile-adduct products via quinone methide form [44]. As shown in Fig. 6, the quinone methide form would immediately accept nucleophilic addition reaction with H_2O molecule, following ring-opening reaction and

further hydrolytic degradation in the ring C, and eventually produced a stable product 2,4-dihydroxybenzoic acid derived from the ring B in the reaction buffer. In addition, Fuentes *et al.* reported that the quinone methide form intermediates ring-opening reaction in the ring C in oxidative conversion of quercetin [45]. This report is consistent with our proposed mechanism.

We conclude that Cu(I)-hydroperoxide derived from the reaction of Cu(I) with H_2O_2 probably participates in morin-induced DNA damage in the presence of Cu(II). It is well known that Cu(II) accelerates aggregation of amyloid β-peptide [46, 47]. On the other hand, Hanaki *et al.* reported that the hydroxyl group at position 2' in ring B of flavonoids, including morin, was particularly important for the inhibition of amyloid β-peptide aggregation [48]. Though morin has the potency to inhibit the aggregation of amyloid β-peptide, our results indicate that morin causes oxidative DNA damage in the presence of Cu(II). Further studies are needed to demonstrate the oxidative pathway of morin in the presence of Cu(II) in view of biomedical applications of morin for Alzheimer's disease.

Acknowledgments

This work was supported by JSPS KAKENHI Grant Numbers JP26293148,

JP15K15237, JP26390017.

Disclosure statement

The authors report no conflicts of interest. The authors alone are responsible for the content and writing of the paper.

References

1. Lee J, Jin H, Lee WS, et al. Morin, a Flavonoid from Moraceae, Inhibits Cancer Cell Adhesion to Endothelial Cells and EMT by Downregulating VCAM1 and Ncadherin. Asian Pac J Cancer Prev. 2016;17(7):3071-5. PubMed PMID: 27509931.
2. Li G, Lu G, Qi Z, et al. Morin Attenuates Streptococcus suis Pathogenicity in Mice by Neutralizing Suilysin Activity. Front Microbiol. 2017;8:460. doi: 10.3389/fmicb.2017.00460. PubMed PMID: 28373868; PubMed Central PMCID: PMCPMC5357624.
3. Chen ZY, Chan PT, Ho KY, et al. Antioxidant activity of natural flavonoids is governed by number and location of their aromatic hydroxyl groups. Chem Phys Lipids. 1996 Mar 29;79(2):157-63. PubMed PMID: 8640902.
4. Arriagada F, Correa O, Gunther G, et al. Morin Flavonoid Adsorbed on Mesoporous Silica, a Novel Antioxidant Nanomaterial. PLoS One. 2016;11(11):e0164507. doi: 10.1371/journal.pone.0164507. PubMed PMID: 27812111; PubMed Central PMCID: PMCPMC5094702.
5. Zhang R, Kang KA, Piao MJ, et al. Cellular protection of morin against the oxidative stress induced by hydrogen peroxide. Chem Biol Interact. 2009 Jan 15;177(1):21-7. doi: 10.1016/j.cbi.2008.08.009. PubMed PMID: 18793623.
6. Shirai A, Onitsuka M, Maseda H, et al. Effect of polyphenols on reactive oxygen species production and cell growth of human dermal fibroblasts after irradiation with ultraviolet-A light. Biocontrol Sci. 2015;20(1):27-33. doi: 10.4265/bio.20.27. PubMed PMID: 25817810.
7. Vanitha P, Senthilkumar S, Dornadula S, et al. Morin activates the Nrf2-ARE pathway and reduces oxidative stress-induced DNA damage in pancreatic beta cells. Eur J Pharmacol. 2017 Apr 15;801:9-18. doi: 10.1016/j.ejphar.2017.02.026. PubMed PMID: 28216051.
8. Kim JM, Lee EK, Park G, et al. Morin modulates the oxidative stress-induced NF-kappaB pathway through its anti-oxidant activity. Free Radic Res. 2010 Apr;44(4):454-61. doi: 10.3109/10715761003610737. PubMed PMID: 20187708.
9. Lee KM, Lee Y, Chun HJ, et al. Neuroprotective and anti-inflammatory effects of morin in a murine model of Parkinson's disease. J Neurosci Res. 2016 Oct;94(10):865-78. doi: 10.1002/jnr.23764. PubMed PMID: 27265894.
10. MadanKumar P, NaveenKumar P, Devaraj H, et al. Morin, a dietary flavonoid, exhibits anti-fibrotic effect and induces apoptosis of activated hepatic stellate cells by suppressing canonical NF-kappaB signaling. Biochimie. 2015 Mar;110:107-18. doi:

10.1016/j.biochi.2015.01.002. PubMed PMID: 25577997.

11. Lemkul JA, Bevan DR. Morin inhibits the early stages of amyloid beta-peptide aggregation by altering tertiary and quaternary interactions to produce "off-pathway" structures. Biochemistry. 2012 Jul 31;51(30):5990-6009. doi: 10.1021/bi300113x. PubMed PMID: 22762350.
12. Hardy J, Chartier-Harlin MC, Mullan M. Alzheimer disease: the new agenda. Am J Hum Genet. 1992 Mar;50(3):648-51. PubMed PMID: 1539602; PubMed Central PMCID: PMCPMC1684301.
13. Sharma D, Singh M, Kumar P, et al. Development and characterization of morin hydrate loaded microemulsion for the management of Alzheimer's disease. Artif Cells Nanomed Biotechnol. 2017 Jan 19:1-14. doi: 10.1080/21691401.2016.1276919. PubMed PMID: 28102083.
14. Sahu SC, Gray GC. Lipid peroxidation and DNA damage induced by morin and naringenin in isolated rat liver nuclei. Food Chem Toxicol. 1997 May;35(5):443-7. PubMed PMID: 9216742.
15. Roy AS, Samanta SK, Ghosh P, et al. Cell cytotoxicity and serum albumin binding capacity of the morin-Cu(ii) complex and its effect on deoxyribonucleic acid. Mol Biosyst. 2016 Aug 16;12(9):2818-33. doi: 10.1039/c6mb00344c. PubMed PMID: 27345944.
16. Hardigree AA, Epler JL. Comparative mutagenesis of plant flavonoids in microbial systems. Mutat Res. 1978 Nov;58(2-3):231-9. PubMed PMID: 370575.
17. Brown JP, Dietrich PS. Mutagenicity of plant flavonols in the Salmonella/mammalian microsome test: activation of flavonol glycosides by mixed glycosidases from rat cecal bacteria and other sources. Mutat Res. 1979 Mar;66(3):223-40. PubMed PMID: 375081.
18. Kasai H, Chung MH, Jones DS, et al. 8-Hydroxyguanine, a DNA adduct formed by oxygen radicals: its implication on oxygen radical-involved mutagenesis/carcinogenesis. J Toxicol Sci. 1991 Feb;16 Suppl 1:95-105. PubMed PMID: 1656061.
19. Oikawa S, Yamada K, Yamashita N, et al. N-acetylcysteine, a cancer chemopreventive agent, causes oxidative damage to cellular and isolated DNA. Carcinogenesis. 1999 Aug;20(8):1485-90. PubMed PMID: 10426796.
20. Serrano M, Hannon GJ, Beach D. A new regulatory motif in cell-cycle control causing specific inhibition of cyclin D/CDK4. Nature. 1993 Dec 16;366(6456):704-7. doi: 10.1038/366704a0. PubMed PMID: 8259215.
21. Oikawa S, Murakami K, Kawanishi S. Oxidative damage to cellular and isolated DNA by homocysteine: implications for carcinogenesis. Oncogene. 2003 Jun 05;22(23):3530-8. doi: 10.1038/sj.onc.1206440. PubMed PMID: 12789261.
22. Kawanishi S, Yamamoto K. Mechanism of site-specific DNA damage induced by

methylhydrazines in the presence of copper(II) or manganese(III). Biochemistry. 1991 Mar 26;30(12):3069-75. PubMed PMID: 1848785.

23. Yamamoto K, Kawanishi S. Site-specific DNA damage induced by hydrazine in the presence of manganese and copper ions. The role of hydroxyl radical and hydrogen atom. J Biol Chem. 1991 Jan 25;266(3):1509-15. PubMed PMID: 1846358.
24. Maxam AM, Gilbert W. Sequencing end-labeled DNA with base-specific chemical cleavages. Methods Enzymol. 1980;65(1):499-560. PubMed PMID: 6246368.
25. Kasai H, Crain PF, Kuchino Y, et al. Formation of 8-hydroxyguanine moiety in cellular DNA by agents producing oxygen radicals and evidence for its repair. Carcinogenesis. 1986 Nov;7(11):1849-51. PubMed PMID: 3769133.
26. Ito K, Inoue S, Yamamoto K, et al. 8-Hydroxydeoxyguanosine formation at the 5' site of 5'-GG-3' sequences in double-stranded DNA by UV radiation with riboflavin. J Biol Chem. 1993 Jun 25;268(18):13221-7. PubMed PMID: 8390459.
27. Pryor WA, Tang RH. Ethylene formation from methional. Biochem Biophys Res Commun. 1978 Mar 30;81(2):498-503. PubMed PMID: 666768.
28. Northrop JH. The Kinetics of the Decomposition of Peroxide by Catalase. J Gen Physiol. 1925 Jan 20;7(3):373-87. PubMed PMID: 19872144; PubMed Central PMCID: PMCPMC2140704.
29. Rapisarda VA, Volentini SI, Farias RN, et al. Quenching of bathocuproine disulfonate fluorescence by Cu(I) as a basis for copper quantification. Anal Biochem. 2002 Aug 01;307(1):105-9. PubMed PMID: 12137786.
30. Burrows CJ, Muller JG. Oxidative Nucleobase Modifications Leading to Strand Scission. Chem Rev. 1998 May 7;98(3):1109-1152. PubMed PMID: 11848927.
31. Geierstanger BH, Kagawa TF, Chen SL, et al. Base-specific binding of copper(II) to Z-DNA. The 1.3-A single crystal structure of d(m5CGUAm5CG) in the presence of CuCl2. J Biol Chem. 1991 Oct 25;266(30):20185-91. PubMed PMID: 1939079.
32. Froystein NA, Davis JT, Reid BR, et al. Sequence-selective metal ion binding to DNA oligonucleotides. Acta Chem Scand. 1993 Jul;47(7):649-57. PubMed PMID: 8363924.
33. Rowley DA, Halliwell B. Superoxide-dependent and ascorbate-dependent formation of hydroxyl radicals in the presence of copper salts: a physiologically significant reaction? Arch Biochem Biophys. 1983 Aug;225(1):279-84. PubMed PMID: 6311105.
34. Kawanishi S, Oikawa S, Murata M, et al. Site-specific oxidation at GG and GGG sequences in double-stranded DNA by benzoyl peroxide as a tumor promoter. Biochemistry. 1999 Dec 21;38(51):16733-9. PubMed PMID: 10606504.
35. Kobayashi H, Oikawa S, Umemura S, et al. Mechanism of metal-mediated DNA damage and apoptosis induced by 6-hydroxydopamine in neuroblastoma SH-SY5Y cells. Free

Radic Res. 2008 Jul;42(7):651-60. doi: 10.1080/10715760802270334. PubMed PMID: 18654880.

36. Min K, Ebeler SE. Flavonoid effects on DNA oxidation at low concentrations relevant to physiological levels. Food Chem Toxicol. 2008 Jan;46(1):96-104. doi: 10.1016/j.fct.2007.07.002. PubMed PMID: 17707569.

37. Yamamoto K, Kawanishi S. Hydroxyl free radical is not the main active species in site-specific DNA damage induced by copper (II) ion and hydrogen peroxide. J Biol Chem. 1989 Sep 15;264(26):15435-40. PubMed PMID: 2549063.

38. Oikawa S, Kawanishi S. Site-specific DNA damage induced by NADH in the presence of copper(II): role of active oxygen species. Biochemistry. 1996 Apr 09;35(14):4584-90. doi: 10.1021/bi9527000. PubMed PMID: 8605209.

39. Oikawa S, Kawanishi S. Distinct mechanisms of site-specific DNA damage induced by endogenous reductants in the presence of iron(III) and copper(II). Biochim Biophys Acta. 1998 Jul 30;1399(1):19-30. PubMed PMID: 9714716.

40. Oikawa S, Hirosawa I, Hirakawa K, et al. Site specificity and mechanism of oxidative DNA damage induced by carcinogenic catechol. Carcinogenesis. 2001 Aug;22(8):1239-45. PubMed PMID: 11470755.

41. Prutz WA. The interaction between hydrogen peroxide and the DNA-Cu(I) complex: effects of pH and buffers. Z Naturforsch C. 1990 Nov-Dec;45(11-12):1197-206. PubMed PMID: 1965680.

42. Dizdaroglu M, Aruoma OI, Halliwell B. Modification of bases in DNA by copper ion-1,10-phenanthroline complexes. Biochemistry. 1990 Sep 11;29(36):8447-51. PubMed PMID: 2123717.

43. Oikawa S, Furukawaa A, Asada H, et al. Catechins induce oxidative damage to cellular and isolated DNA through the generation of reactive oxygen species. Free Radic Res. 2003 Aug;37(8):881-90. PubMed PMID: 14567448.

44. Kummer S, Ruth W, Kragl U. Oxidation of Flavonols in an Electrochemical Flow Cell Coupled Online with ESI-MS. Electroanal. 2016 May;28(5):990-997. doi: 10.1002/elan.201501055. PubMed PMID: WOS:000379040500011; English.

45. Fuentes J, Atala E, Pastene E, et al. Quercetin Oxidation Paradoxically Enhances its Antioxidant and Cytoprotective Properties. J Agr Food Chem. 2017 Dec 20;65(50):11002-11010. doi: 10.1021/acs.jafc.7b05214. PubMed PMID: WOS:000418783400019; English.

46. Atwood CS, Moir RD, Huang X, et al. Dramatic aggregation of Alzheimer abeta by Cu(II) is induced by conditions representing physiological acidosis. J Biol Chem. 1998 May 22;273(21):12817-26. PubMed PMID: 9582309.

47. Bin Y, Li X, He Y, et al. Amyloid-beta peptide (1-42) aggregation induced by copper ions under acidic conditions. Acta Biochim Biophys Sin (Shanghai). 2013 Jul;45(7):570-7. doi: 10.1093/abbs/gmt044. PubMed PMID: 23747389.
48. Hanaki M, Murakami K, Akagi K, et al. Structural insights into mechanisms for inhibiting amyloid beta42 aggregation by non-catechol-type flavonoids. Bioorg Med Chem. 2016 Jan 15;24(2):304-13. doi: 10.1016/j.bmc.2015.12.021. PubMed PMID: 26719209.

Figure legends

Fig. 1. Autoradiograms of ^{32}P-5'-end-labeled DNA fragments incubated with morin in the presence of Cu(II).
Reaction mixtures contained the ^{32}P-5'-end-labeled 328 bp fragment, 100 μM/base calf thymus DNA, the indicated concentrations of morin, and 20 μM $CuCl_2$ in 4 mM sodium phosphate buffer (pH 7.8) containing 5 μM DTPA. After incubation at 37 ºC for 5 hr, the DNA fragment was treated A) with, or B) without, piperidine and electrophoresed on a polyacrylamide gel.

Fig. 2. Effects of scavengers on morin-induced DNA damage in the presence of Cu(II).
Reaction mixtures contained the ^{32}P-5'-end-labeled 328 bp fragment, 100 μM/base calf thymus DNA, 50 μM morin, each scavenger or bathocuproine, and 20 μM $CuCl_2$ in 4 mM sodium phosphate buffer (pH 7.8) containing 5 μM DTPA. After incubation at 37 ºC for 5 hr, the DNA fragment was treated with piperidine and electrophoresed on a polyacrylamide gel. The concentration of each scavenger and bathocuproine were as follows: 0.8 M ethanol (EtOH), 0.1 M mannitol, 0.1 M sodium formate, 1.0 M methional, 30 U catalase, 50 μM bathocuproine, and 30 U superoxide dismutase (SOD).

Fig. 3. Site specificity of morin-induced DNA cleavage in the presence of Cu(II).
Reaction mixtures contained the ^{32}P-5'-end-labeled A) 147 bp fragment or B) 309 bp fragment, 100 μM/base calf thymus DNA, 500 μM morin, and 20 μM $CuCl_2$ in 4 mM sodium phosphate buffer (pH 7.8) containing 5 μM DTPA. After incubation at 37 ºC for 5 hr, the DNA fragment was treated with piperidine and electrophoresed on a polyacrylamide gel. Abbreviations indicate each DNA base, A: adenine, T: thymine, G: guanine, C: cytosine.

Fig. 4. Formation of 8-oxodG in calf thymus DNA induced by morin in the presence of Cu(II).
Calf thymus DNA fragments of 100 μM/base were incubated with indicated concentrations of morin in the presence of 20 μM $CuCl_2$ in 4 mM sodium phosphate buffer (pH 7.8) containing 5 μM DTPA at 37ºC for 1 hr. After ethanol precipitation, the

DNA was digested to nucleosides with nuclease P_1 and calf intestine phosphatase, then analyzed with an HPLC-ECD. In order to clarify the mechanism of autoxidation, dissolved oxygen in the reaction mixture containing morin and Cu(II) was removed by bubbling nitrogen gas for 1 min (hypoxic conditions), after which 8-oxodG was determined. Results are expressed as mean of values obtained from two independent experiments.

Fig. 5. Analysis of reaction products by morin in the presence of Cu(II).
(A) HPLC chromatograms of oxidized products of morin after reaction at 37 ºC for 21 hr. Reaction mixture consisted 500 µM of morin and (a) 0 µM, (b) 20 µM, or (c) 200 µM of $CuCl_2$ in 4 mM sodium phosphate buffer (pH 7.8) containing 5 µM DTPA. (B) ^{1}H- and ^{13}C-NMR spectra of the major oxidized product (Rt 14.8 min) were recorded in DMSO-d_6 at 20 ºC. In the ^{1}H-NMR chart, integral values corresponding each proton were indicated under the scale bar of chemical shift. (C) Estimated chemical structure of the oxidized product generated by morin and Cu(II).

Fig. 6. A possible mechanism of oxidative DNA damage induced by morin in the presence of Cu(II).

Fig. 1

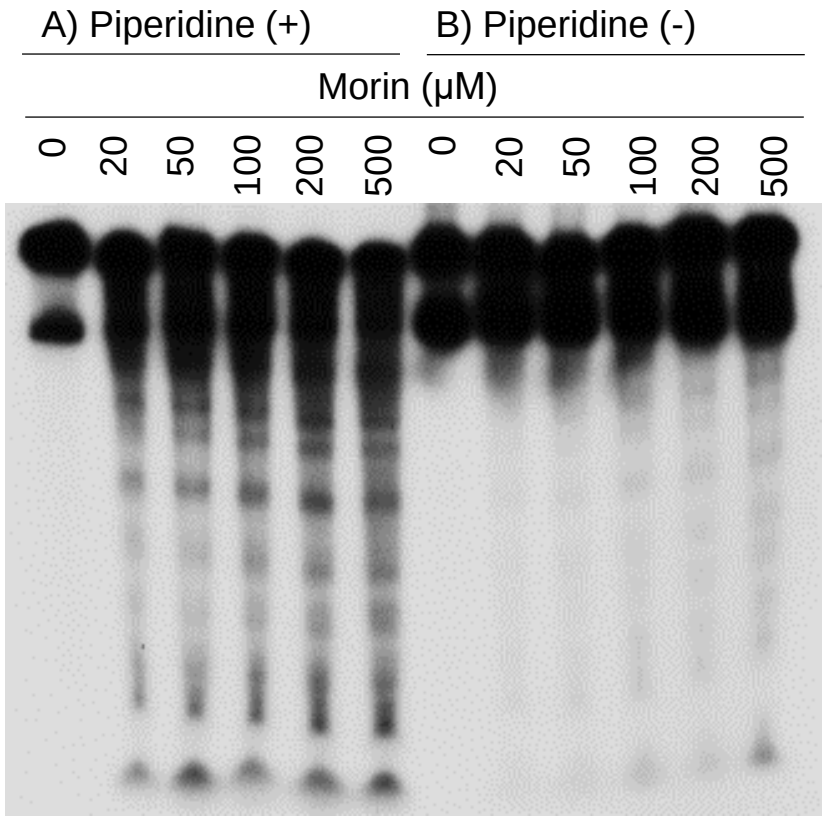
A) Piperidine (+)
B) Piperidine (-)
Morin (μM)
0
20
50
100
200
500
0
20
50
100
200
500

Fig. 2

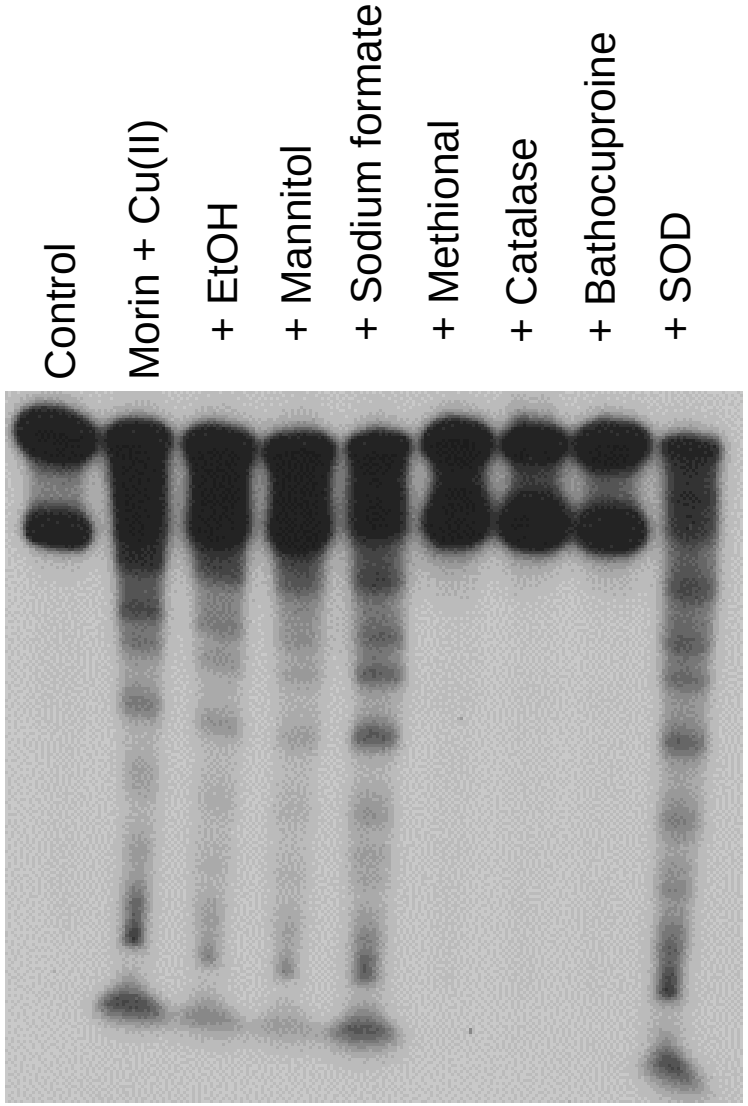
Control
Morin + Cu(II)
+ EtOH
+ Mannitol
+ Sodium formate
+ Methional
+ Catalase
+ Bathocuproine
+ SOD

Fig. 3

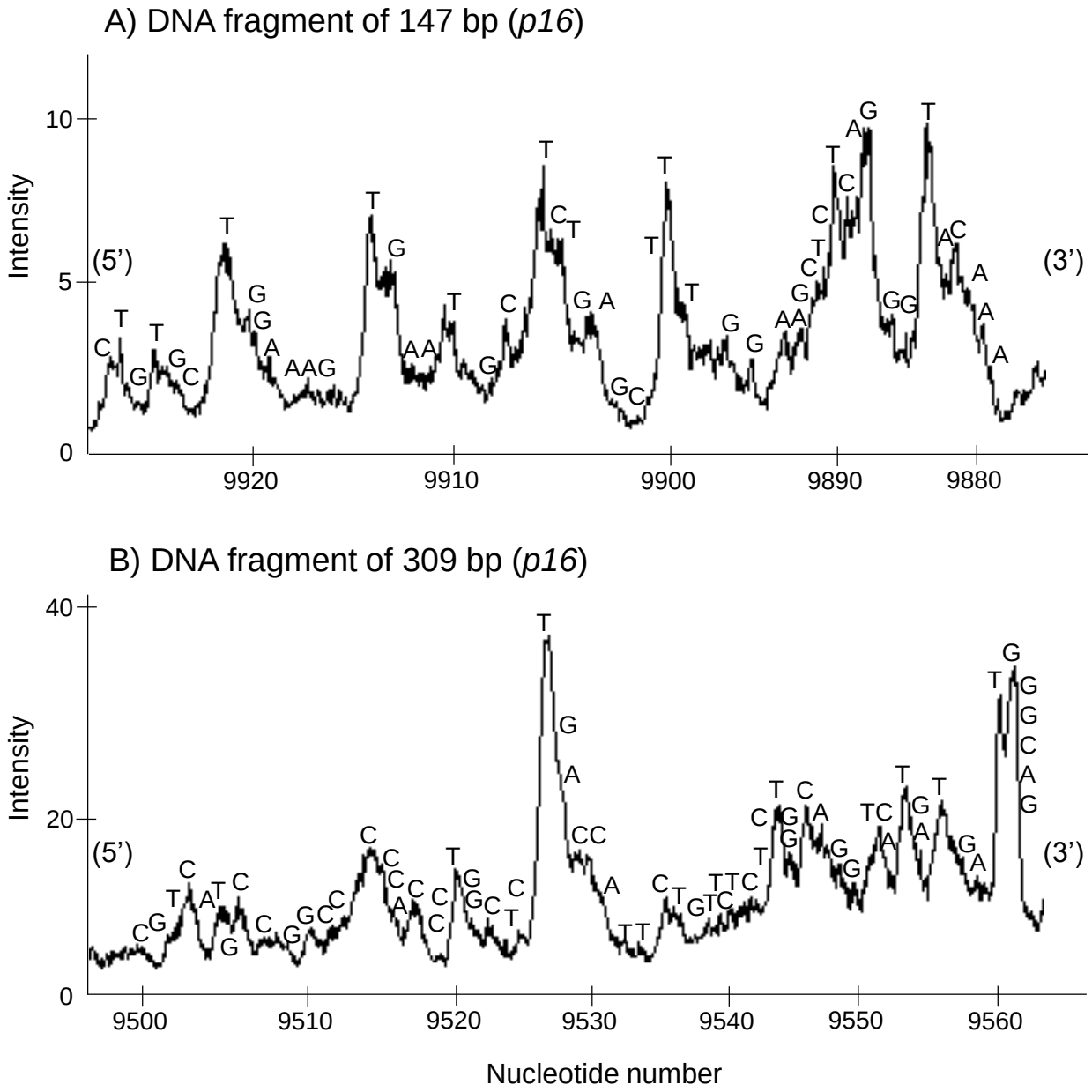
A) DNA fragment of 147 bp (*p16*)
Intensity
10
5
0
(5')
(3')
9920
9910
9900
9890
9880
B) DNA fragment of 309 bp (*p16*)
Intensity
40
20
0
(5')
(3')
9500
9510
9520
9530
9540
9550
9560
Nucleotide number

Fig. 4

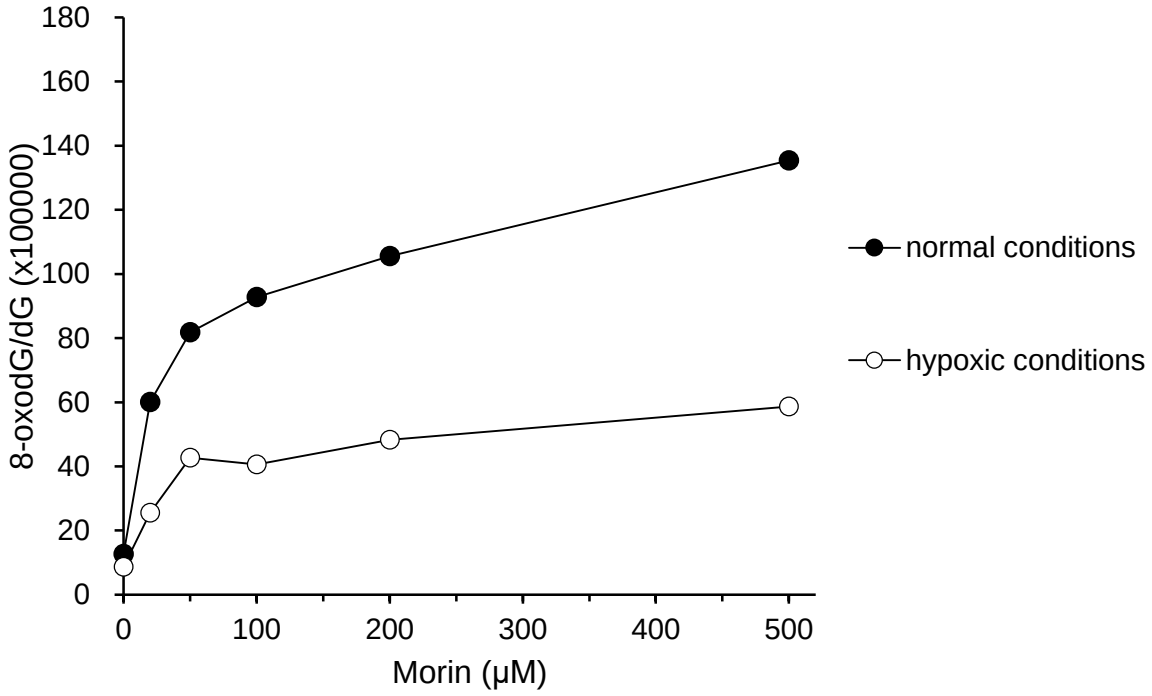
180
160
140
120
100
80
60
40
20
0
8-oxodG/dG (x100000)
0
100
200
300
400
500
Morin (μM)
normal conditions
hypoxic conditions

Fig. 5

A)

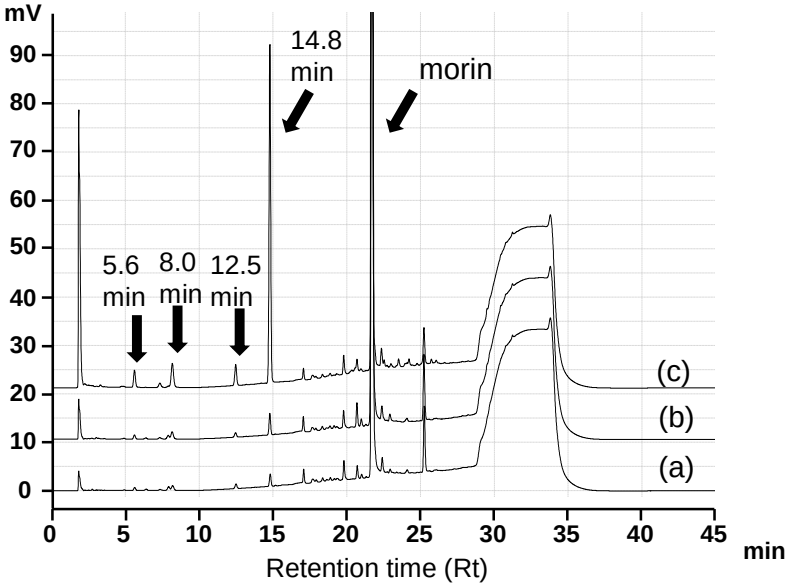

B-1) <u>^{1}H-NMR in DMSO-d_6, 600 MHz</u>

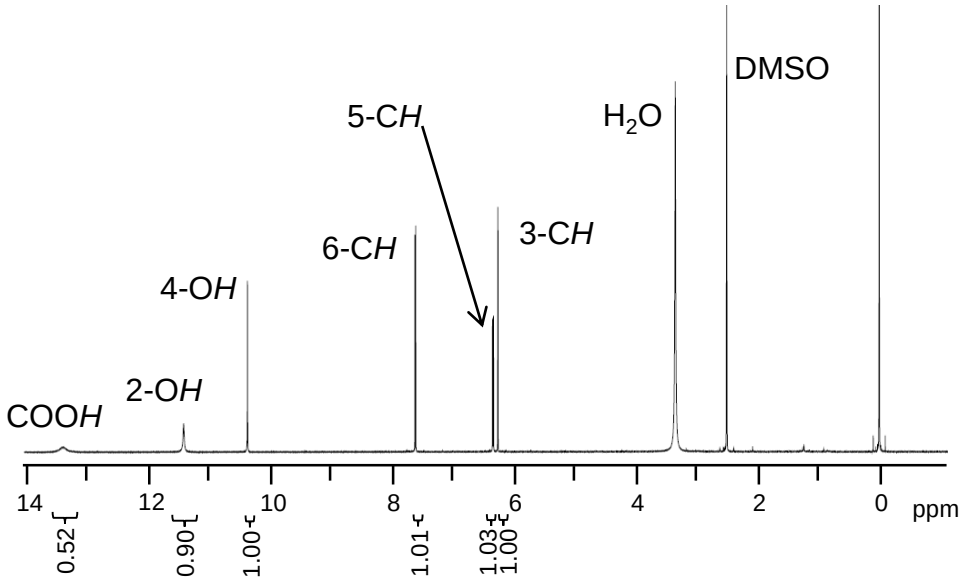

B-2) <u>^{13}C-NMR in DMSO-d_6, 150 MHz</u>

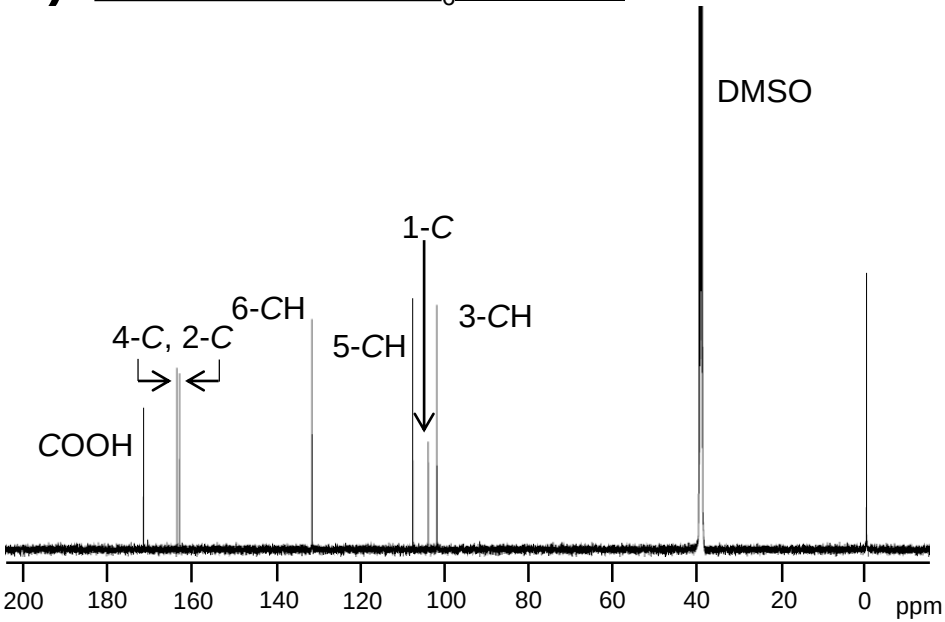

C)

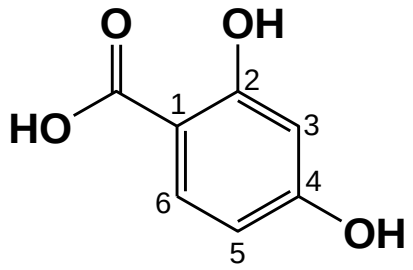

2,4-dihydroxybenzoic acid

Fig. 6

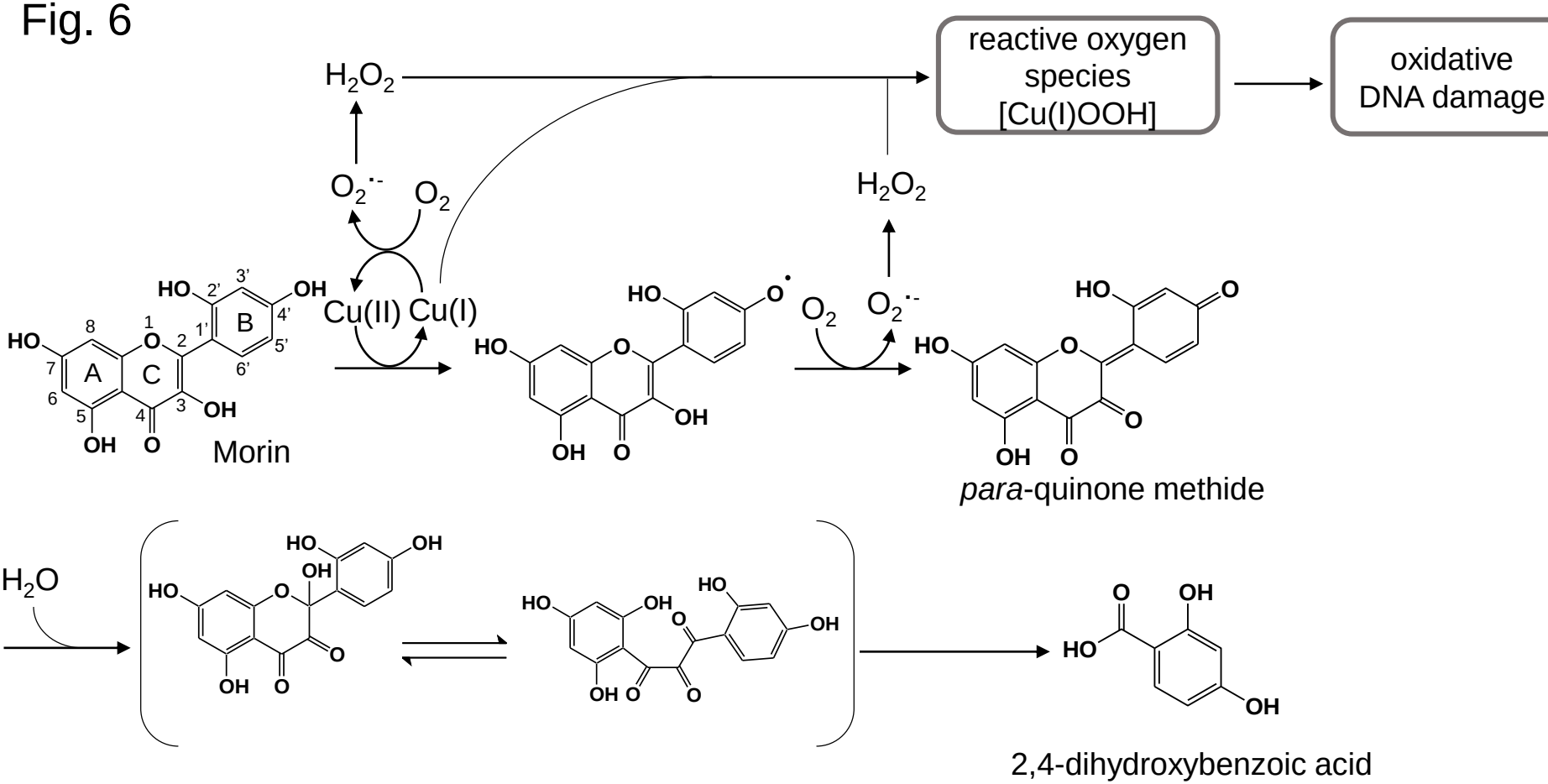
H_2O_2
reactive oxygen species [Cu(I)OOH]
oxidative DNA damage
$O_2^{\cdot-}$
O_2
Cu(II) Cu(I)
H_2O_2
Morin
para-quinone methide
H_2O
2,4-dihydroxybenzoic acid